Exchange of orbital angular momentum of light via noise-induced coherence

Seyyed Hossein Asadpour,[1,*] Ziauddin,[2,†] Muqaddar Abbas,[3,‡] and Hamid R. Hamedi[4,§]

[1]*Department of Physics, Iran University of Science and Technology, 1684613114 Tehran, Iran*

[2]*Quantum Optics Laboratory, Department of Physics, COMSATS University, Islamabad, Pakistan*

[3]*Ministry of Education Key Laboratory for Nonequilibrium Synthesis and Modulation of Condensed Matter, Shaanxi Province Key Laboratory of Quantum Information and Quantum Optoelectronic Devices, School of Physics, Xi'an Jiaotong University, Xi'an 710049, China*

[4]*Institute of Theoretical Physics and Astronomy, Vilnius University, Sauletekio 3, Vilnius 10257, Lithuania*

(Received 2 August 2021; revised 11 January 2022; accepted 28 February 2022; published 16 March 2022)

The noise-induced coherence created via the quantum interference of incoherent radiation in atomic three-level systems of V and Λ types driven by a pair of weak laser pulses is shown to result in exchange of optical vortices. In the three- level V-type atom-light coupling the system is populated in its ground level, while in the Λ model the system is initially prepared in an electromagnetically induced transparency state. By solving the quantum optical Maxwell-Bloch equations and with quantum interference of incoherent radiation present, we show that the orbital angular momentum (OAM) of the vortex probe beam can be transferred to a generated signal field. While the exchange efficiency in the V configuration is higher, the losses are less in the Λ scheme when we consider such a noise-induced coherence. We further discuss the effects of phase mismatching and inhomogeneous broadening on the energy conversion between light beams carrying OAM.

DOI: 10.1103/PhysRevA.105.033709

I. INTRODUCTION

Quantum coherence and interference in multilevel quantum systems lead to many novel and unexpected phenomena such as electromagnetically induced transparency (EIT) [1,2], lasing without population inversion [3], creation of optical solitons [4–7], and four-wave mixing (FWM) [8–10]. It is important to prepare the atomic configurations in order for these coherent phenomena to appear; however, the incoherent radiation usually plays a destructive role (noise) in the creation of this coherence. There have been several attempts in which coherence induced from such noises is employed for the preparation of the atoms [11–14]. The coherence induced by interference of incoherent radiation has been used to control the optical bistability [14], lasing without population inversion [15], quenching of spontaneous emission [16], and others [17–19].

Light beams can carry an orbital angular momentum (OAM) [20]. This feature provides additional features for the coherent control of light as it illustrates another degree of freedom suitable for applications in the quantum computation, quantum teleportation, and quantum information storage [21–24]. When interacting with atoms, such optical vortex beams result in different phenomena, including light-induced torque [25,26], atom vortex beams [27], entanglement of OAM states of photon pairs [28], OAM-based FWM [29–35], spatially dependent optical transparency [36,37], and the vortex slow light [38]. The twisted slow light [39] gives additional possibilities in coherent manipulation of the optical information during the storage and readout of the slow light [40].

In previous theoretical studies on interplay of optical vortices with atoms a situation has been considered in which the atoms are initially in their ground states with the Rabi frequency of the control fields much stronger than that of the probe field. The OAM of the control vortex beam has been illustrated to be transferred to the weak probe beam in the tripod scheme during the storage and retrieval of the probe field [41]. The transfer of optical vortices can take also place without switching off and on of the control fields (without storage and retrieval of the probe field), by applying a pair of weaker probe fields in the closed-loop four-level double-Λ schemes [30,42]. It has been also shown that the exchange of optical vortices in non–closed-loop Λ-type configuration is possible under the condition of weak atom-light interaction in coherently prepared atomic media [43]. In such a case, the atoms are initially populated in a coherent superposition of the lower atomic levels. If a single vortex beam initially shines on one transition of the scheme, an additional laser beam is generated with the same OAM as that of the incident vortex beam. The absorption of the incident probe beam appears mostly at the beginning of the atomic medium within the absorption length. The losses disappear as the probe beam propagates deeper into the medium where the atoms are transferred to their dark states.

Following the models proposed in Refs. [13,15], we consider now two different situations in V- and Λ-type quantum systems in order for exchanging the optical vortices via coherence induced by incoherent pumping radiation noise. In the V-type atomic system the system is initially populated in the

*S.Hosein.Asadpour@gmail.com
†Ziauddin@ comsats.edu.pk
‡muqaddarabbas@xjtu.edu.cn
§hamid.hamedi@tfai.vu.lt

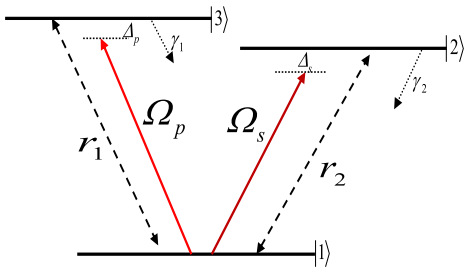

FIG. 1. Schematic of three-level V-type atomic system with closely spaced upper states. r_1 and r_2 are pump rates; Ω_p and Ω_s are probe and signal fields.

ground level while in the Λ-type quantum system the system populated in the EIT ground state. It is found that the OAM exchange can take place in both schemes when the quantum interference is taken into account. However, the swapping of OAM is accompanied by strong losses in the V scheme. The effects of phase mismatching and inhomogeneous broadening on the energy conversion between light beams carrying OAM have been also discussed.

II. MODEL AND THEORY

A. V-type atomic system

We consider first a three-level system in a so-called V scheme interacting with a pair of Rabi frequencies Ω_p and Ω_s as illustrated in Fig. 1. Two closely spaced doublets $|3\rangle$ and $|2\rangle$ are coupled by two light fields to the ground state $|1\rangle$ via probe and signal fields Ω_p and Ω_s, respectively. The upper levels decay into the ground level with the rates γ_1 and γ_2, respectively. An incoherent pumping field R with pumping rates r_1 and r_2 is applied between lower level $|1\rangle$ to doublet levels $|2\rangle$ and $|3\rangle$. We suppose that one polarized broadband field can couple with more than one transition. Therefore the interference from incoherent pumping fields may arrise.

Generally, three main dynamical processes may occur in the system, including incoherent pump processes through r_1, r_2, interaction of the atomic system with coherent fields, and interaction with the reservoir governing the decay processes from levels $|3\rangle$ and $|2\rangle$ to ground level $|1\rangle$. We charactrize theses processes by interaction terms H_R, H_A, and H_γ, respectively.

In the interaction picture, the Hamiltonian can be written as the sum of these three terms,

$$H = H_R + H_A + H_\gamma. \tag{1}$$

The first term represents incoherent pump processes modeled via the interaction of the atomic system with the incoherent radiation R:

$$H_R = \mu_{21} R|2\rangle\langle 1| + \mu_{31} R|3\rangle\langle 1| + \text{H.c.} \tag{2}$$

Note that the spectrum of the field covers both upper levels simultaneously; as a result, one and the same field drives both transitions. One can characterize these transitions by dipole matrix elements μ_{21} and μ_{31} and transition frequencies ω_{21} and ω_{31}. The incoherent field has δ-like correlation at different times, i.e.,

$$\langle R^*(t)R(t')\rangle = \Re\delta(t-t'). \tag{3}$$

One can show the effect of H_R through the pumping parameter $r_{1,2} = 2(\mu^2_{21,31}/\hbar^2)\Re$. It should be pointed out that these correlations are not expected to cover the whole range of frequencies. It is sufficient that they are at least approximately valid in the vicinity of both resonances and cover the frequency seperation of two upper levels.

The next term in Eq. (1), H_A, which is the interaction Hamiltonian of the system with Rabi frequencies $\Omega_{p(s)} = \mu_{31(21)}E_{p(s)}/\hbar$ and detuning $\Delta_{p(s)}$, reads

$$\begin{aligned} H_A = {} & \hbar(\Delta_p|3\rangle\langle 3| + \Delta_s|2\rangle\langle 2|) \\ & + \hbar(\Omega_p|3\rangle\langle 1| + \Omega_s|2\rangle\langle 1| + \text{H.c.}). \end{aligned} \tag{4}$$

The last term in Eq. (1) denotes the interaction with the reservoir of vacuum oscillators. The specified Hamiltonian of this term is given by

$$\begin{aligned} H_\gamma = {} & -\hbar\sum_k g_k^{(1)} e^{-i\nu_k t}|3\rangle\langle 1|\hat{a}_k \\ & -\hbar\sum_k g_k^{(2)} e^{-i\nu_k t}|2\rangle\langle 1|\hat{a}_k + \text{H.c.}, \end{aligned} \tag{5}$$

where $g_k^{(1,2)}$ represent the coupling constant between the kth vacuum mode and the atomic transitions from $|2\rangle$ and $|3\rangle$ to $|1\rangle$, $\hat{a}_k(\hat{a}_k^\dagger)$ is the annihilation (creation) operator of a photon in the kth vacuum mode, which obey the conventional bosonic communication rule $[\hat{a}_k, \hat{a}_{k'}^\dagger] = \delta_{kk'}$.

To model the quantum dynamics of the V-type atomic system driven by coherent and incoherent radiation, one can consider the interaction terms separately to obtain the corresponding terms in the density-matrix equations. The influence of the interaction potentials on the density matrix can be obtained by means of the Liouville equation:

$$\begin{aligned} \dot{\rho}^{(R,A,\gamma)} &= -\frac{i}{\hbar}[H_{R,A,\gamma}(t), \rho^{(R,A,\gamma)}(t)] \\ &= -\frac{i}{\hbar}[H_{R,A,\gamma}(t)\rho^{(R,A,\gamma)}(t) - \rho^{(R,A,\gamma)}(t)H_{R,A,\gamma}(t)]. \end{aligned} \tag{6}$$

The complete density matrix has been reduced here to different parts as $\rho = \rho^{(R)} + \rho^{(A)} + \rho^{(\gamma)}$, coupling only to the corresponding part of the Hamiltonian. The interaction Hamiltonians H_A is straightforward to obtain. Yet, those related to the interference effects (i.e., H_R and H_γ) are quite complicated to derive (see Appendixes A and B). Transforming to a rotated frame and including all the atomic decays as shown in Fig. 1, the resulting density-matrix equations are

$$\begin{aligned} \dot{\rho}_{31} = {} & -\left[\frac{1}{2}(\gamma+3r) + i\Delta_p\right]\rho_{31} - i\Omega_p(\rho_{33}-\rho_{11}) \\ & - i\Omega_s\rho_{32} - \frac{\eta r}{2}\rho_{21}, \\ \dot{\rho}_{21} = {} & -\left[\frac{1}{2}(\gamma+3r) + i\Delta_s\right]\rho_{21} - i\Omega_p\rho_{23} \\ & + i\Omega_s(\rho_{11}-\rho_{22}) - \frac{\eta r}{2}\rho_{31}, \end{aligned} \tag{7}$$

where we have set $r_1 = r_2 = r$, and $\gamma_1 = \gamma_2 = \gamma$. The interference term η containing the products of pump rates is central to our discussion. This factor is the normalized scalar product of corresponding dipole matrix elements:

$$\eta = \frac{\mu_{31}\mu_{21}}{|\mu_{31}||\mu_{21}|}. \tag{8}$$

In principle the dipole moments μ_{31} and μ_{21} have different directions. When the two electric dipole moments are parallel the interference is maximum ($\eta = 1$), while for the perpendicular electric dipole moments the interference term vanishes ($\eta = 0$).

In what follows, we solve Eq. (7) in the weak-field approximation, where the intensities of the probe and signal fields are sufficiently weak. Within the weak-field approximation, we can apply the perturbation approach to the density-matrix equations, which is introduced in terms of the perturbation expansion

$$\rho_{ij} = \rho_{ij}^{(0)} + \lambda\rho_{ij}^{(1)} + \lambda^2\rho_{ij}^{(2)} + \cdots, \quad (i, j = 1, 2, 3), \tag{9}$$

where λ describes a continuously varying parameter ranging from zero to unity. It should be pointed out that here $\rho_{ij}^{(0)}$, $\rho_{ij}^{(1)}$, and $\rho_{ij}^{(2)}$ are of the zeroth, first, and second orders in weak fields. In the limit of the weak-field approximation, the atom is predominantly populated in the initial ground state $|1\rangle$. This indicates that, for the zeroth-order density-matrix elements $\rho_{11}^{(0)} = 1$ but $\rho_{ij}^{(0)} = 0 (i \neq 0, j \neq 0)$. Due to the fact that the fields are sufficiently weak, only the first-order terms are important. Therefore, we only keep the first order in the probe and signal fields. Using this condition and substituting Eq. (9) into Eq. (7), the equations of motion for the first-order density-matrix elements change to

$$\begin{aligned}
\dot{\rho}_{31}^{(1)} &= -\left[\frac{1}{2}(\gamma + 3r) + i\Delta_p\right]\rho_{31}^{(1)} - \frac{\eta r}{2}\rho_{21}^{(1)} + i\Omega_p, \\
\dot{\rho}_{21}^{(1)} &= -\left[\frac{1}{2}(\gamma + 3r) + i\Delta_s\right]\rho_{21}^{(1)} - \frac{\eta r}{2}\rho_{31}^{(1)} + i\Omega_s.
\end{aligned} \tag{10}$$

After some algebraic calculations, the following off-diagonal density-matrix elements $\rho_{31}^{(1)}$ and $\rho_{21}^{(1)}$ corresponding to weak fields are obtained:

$$\rho_{31}^{(1)} = \frac{i\Delta_{21}}{\Delta_{21}\Delta_{31} - K^2}\Omega_p + \frac{iK}{\Delta_{21}\Delta_{31} - K^2}\Omega_s = a_1\Omega_p + b_1\Omega_s, \tag{11a}$$

$$\rho_{21}^{(1)} = \frac{i\Delta_{31}}{\Delta_{21}\Delta_{31} - K^2}\Omega_s + \frac{iK}{\Delta_{21}\Delta_{31} - K^2}\Omega_p = a_2\Omega_p + b_2\Omega_s, \tag{11b}$$

with $\Delta_{31} = \frac{1}{2}(\gamma + 3r) + i\Delta_p$, $\Delta_{21} = \frac{1}{2}(\gamma + 3r) + i\Delta_s$, $K = \frac{\eta}{2}r$, $a_1 = \frac{i\Delta_{21}}{\Delta_{21}\Delta_{31} - K^2}$, $b_1 = \frac{iK}{\Delta_{21}\Delta_{31} - K^2}$, $a_2 = \frac{iK}{\Delta_{21}\Delta_{31} - K^2}$, and $b_2 = \frac{i\Delta_{31}}{\Delta_{21}\Delta_{31} - K^2}$.

Under the slowly varying envelope approximation and assuming time-independent fields, the Maxwell equations for probe and signal fields Ω_p and Ω_s propagating in the z direction take the form

$$\frac{\partial\Omega_p}{\partial Z} = \frac{i\alpha_p\gamma}{2L}[a_1\Omega_p + b_1\Omega_s], \tag{12a}$$

$$\frac{\partial\Omega_s}{\partial Z} = \frac{i\alpha_s\gamma}{2L}[a_2\Omega_p + b_2\Omega_s]. \tag{12b}$$

Here, α_p and α_s are the optical depths of the corresponding probe and signal fields, and L characterizes the length of the medium. Let us now assume that initially at the beginning of the atomic cloud ($Z = 0$) $\Omega_p(Z = 0) = \Omega_p(0)$ and $\Omega_s(Z = 0) = 0$. Solving the coupled equations (12a) and (12b) for the Rabi frequency of Ω_p and Ω_s, one gets

$$\Omega_s(Z) = \frac{A_2}{A}\Omega_p(0)[e^{\frac{A}{4L}Z} - e^{-\frac{A}{4L}Z}]e^{(\frac{A_1+B_2}{4L}Z)}, \tag{13a}$$

$$\Omega_p(Z) = \frac{A_1 - B_2}{A}\Omega_p(0)e^{(\frac{A_1+B_2}{4L}Z)}\left[\sinh\left(\frac{A}{4L}Z\right) + \frac{A}{A_1 - B_2}\cosh\left(\frac{A}{4L}Z\right)\right], \tag{13b}$$

where

$$A_1 = i\alpha\gamma a_1, \tag{14a}$$

$$B_1 = i\alpha\gamma b_1, \tag{14b}$$

$$A_2 = i\alpha\gamma a_2, \tag{14c}$$

$$B_2 = i\alpha\gamma b_2, \tag{14d}$$

$$A = \sqrt{(A_1 - B_2)^2 + 4A_2B_1}. \tag{14e}$$

Substituting Eqs (13a) and (13b) into Eq. (11b) yields

$$\rho_{21} = a_2\Omega_p(0)e^{(\frac{A_1+B_2}{4L}Z)}\left[\frac{A_1}{A}\sinh\left(\frac{A}{4L}Z\right) + \cosh\left(\frac{A}{4L}Z\right)\right]. \tag{15}$$

By assuming the resonance conditions of the probe and signal fields, i.e., $\Delta_p = \Delta_s = 0$, we have

$$\Omega_p(z) = \frac{1}{2}\Omega_p(0)\left[\exp\left(\frac{\alpha Z}{L}\frac{(\eta - 3)r - \gamma}{(\gamma + 3r)^2 - r^2}\right) + \exp\left(-\frac{\alpha Z}{L}\frac{(\eta + 3)r + \gamma}{(\gamma + 3r)^2 - r^2}\right)\right], \tag{16a}$$

$$\Omega_s(z) = \Omega_p(0)\left[\exp\left(\frac{\alpha Z}{L}\frac{(\eta - 3)r + \gamma}{(\gamma + 3r)^2 - r^2}\right) - \exp\left(-\frac{\alpha Z}{L}\frac{(\eta + 3)r + \gamma}{(\gamma + 3r)^2 - r^2}\right)\right]. \tag{16b}$$

Let us consider the probe field to carry an optical vortex. The Rabi frequency of the probe field is characterized by

$$\Omega_p(0) = \Omega_p = |\Omega_p|\exp\left(\mathrm{i}l_p\Phi\right), \tag{17}$$

where Φ is the azimuthal angle and l_p shows the OAM number. For a Laguerre-Gaussian (LG) doughnut beam we may write

$$|\Omega_p| = \varepsilon_p(r/w)^{|l_p|}\exp\left(-r^2/w^2\right), \tag{18}$$

where r represents the distance from the vortex core (cylindrical radius), w denotes the beam waist parameter, and ε_p is the strength of the vortex beam.

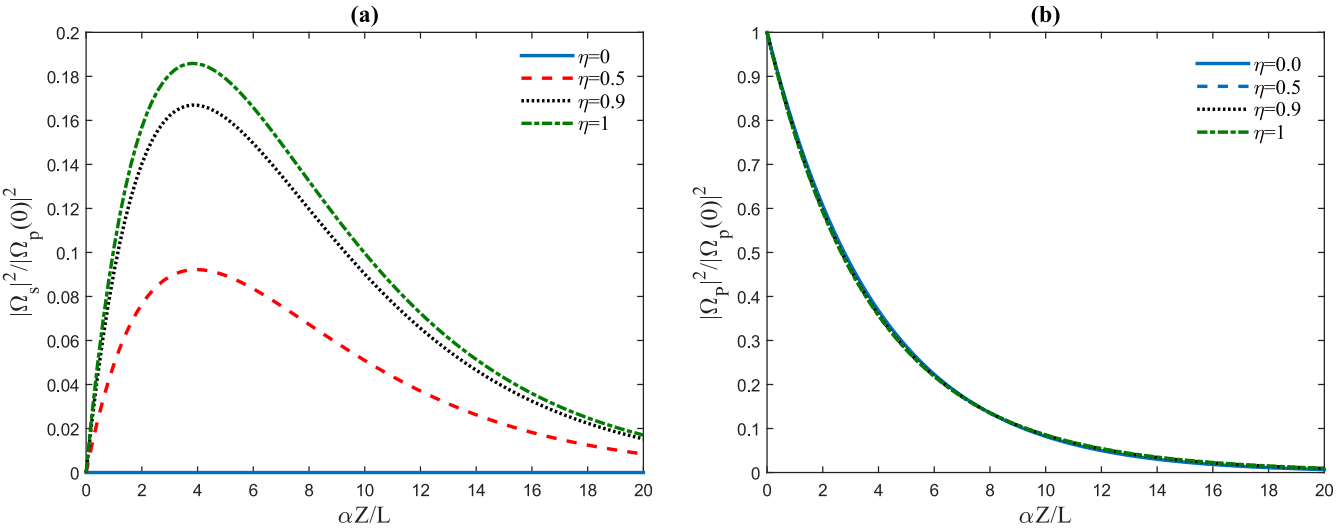

FIG. 2. The dependence of the dimensionless intensity of the signal field $|\Omega_s|^2/|\Omega_p(0)|^2$ (a) and the probe field $|\Omega_p|^2/|\Omega_p(0)|^2$ (b) on the dimensionless distance $\alpha Z/L$. The selected parameters are $\alpha = 20$, $r = 1\gamma$, $\Delta_p = \Delta_s = 0$.

First, we observe that the signal field Ω_s is generated with the same topological charge as the probe field. Second, we consider the efficiency of frequency conversion from the initial beam Ω_p to the generated signal light Ω_s described by Eq. (16b). The dependence of the intensities $|\Omega_s|^2/|\Omega_p(0)|^2$ and $|\Omega_p|^2/|\Omega_p(0)|^2$ on the dimensionless distance $\alpha Z/L$ is shown in Figs. 2(a) and 2(b), respectively, for different values of quantum interference η. As expected, the conversion efficiency governed by $|\Omega_s|^2/|\Omega_p(0)|^2$ is completely zero in the absence of the quantum interference ($\eta = 0$) [see Fig. 2(a)]. One can see that by increasing the quantum interference term η from 0 to 1, the conversion efficiency is enhanced and reaches to 18% for $\eta = 1$ at $\alpha Z \approx 4\,L$. However, when the signal light propagates deeper through the medium the conversion efficiency reduces to a small value. This is attributed to the presence of absorption losses for very large propagation distances which limits the propagation of optical vortices. As observed in Fig. 2(b), the probe vortex beam also experiences absorption losses on propagation.

We look for optimal situations in which the energy conversion efficiency is maximum while simultaneously the absorption losses are minimum. Figure 3 illustrates the variation in space of field intensities $|\Omega_s|^2/|\Omega_p(0)|^2$ and $|\Omega_p|^2/|\Omega_p(0)|^2$ for different values of incoherent pumping rate when the quantum interference term η is set to be maximum ($\eta = 1$). It is seen from Fig. 3(a) that by increasing the incoherent pumping rate, the conversion efficiency is increased. For a particular value $r = 6\gamma$, the exchange efficiency reaches to 24% which is accompanied by negligible energy losses at larger propagation distances. The probe vortex survives longer now for larger incoherent pumping rates, as can be seen in Fig. 3(b).

In Fig. 4, we show the exchange efficiency versus optical depth α for different values of incoherent pumping field when

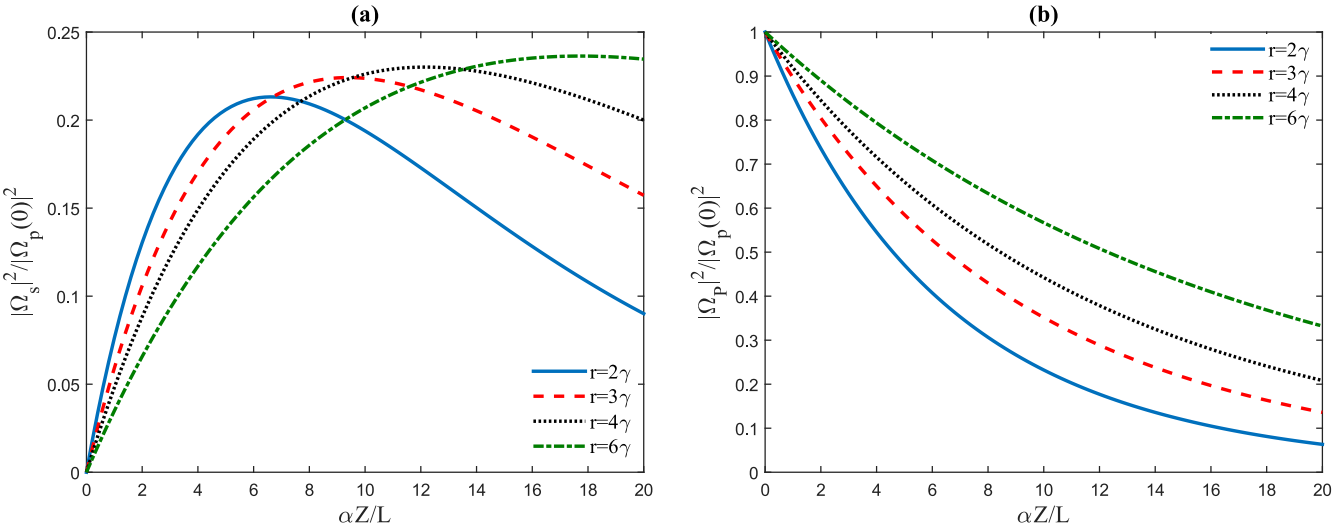

FIG. 3. The dependence of the dimensionless intensity of the signal field $|\Omega_s|^2/|\Omega_p(0)|^2$ (a) and probe field $|\Omega_p|^2/|\Omega_p(0)|^2$ (b) on the dimensionless distance $\alpha Z/L$. The selected parameters are $\alpha = 20$, $\eta = 1$, $\Delta_p = \Delta_s = 0$.

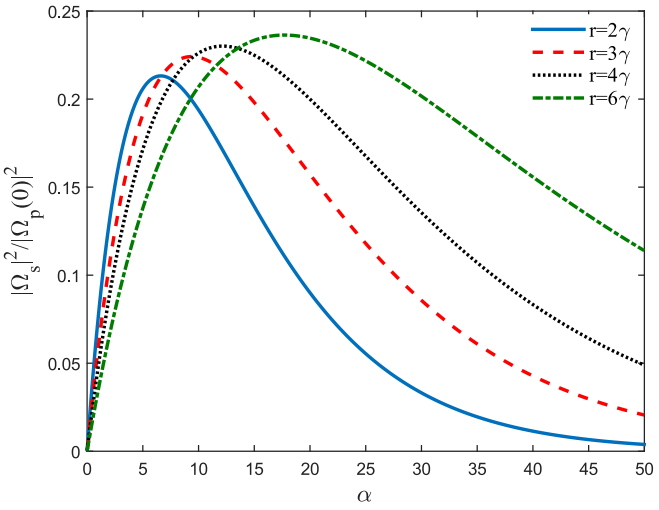

FIG. 4. The dependence of the dimensionless intensity of the signal field $|\Omega_s|^2/|\Omega_p(0)|^2$ on the optical depth α. The selected parameters are $Z = L,\ \eta = 1,\ \Delta_p = \Delta_s = 0$.

the quantum interference term is maximum. We find that the maximum exchange efficiency is possible for $\alpha = 20$ and $r = 6\gamma$. However, by increasing the optical depth α, one can find that the exchange efficiency drops down due to presence of losses in the medium.

B. Λ-Type atomic system

Next we consider a Λ-type three-level atomic system shown in Fig. 5, where the upper state $|3\rangle$ is connected to two lower closely spaced states $|1\rangle$ and $|2\rangle$ by dipole allowed transitions via two light fields Ω_p and Ω_s, respectively.

The incoherent pump field $r_{1(2)}$ drives the two lower states to the same upper state and back. The upper state decays through two different paths to lower states. By the same method as in the previous section we will derive the motion equations of the density-matrix elements for the atomic system:

$$\dot{\rho}_{31} = -\tfrac{1}{2}(2\gamma + 3r + i\Delta_p)\rho_{31} - i\Omega_s\rho_{21} + i\Omega_p(\rho_{33} - \rho_{11}) - \tfrac{1}{2}\eta r\rho_{32}, \tag{19a}$$

$$\dot{\rho}_{32} = -\tfrac{1}{2}(2\gamma + 3r + i\Delta_s)\rho_{32} - i\Omega_p\rho_{12} + i\Omega_s(\rho_{33} - \rho_{22}) - \tfrac{1}{2}\eta r\rho_{31}. \tag{19b}$$

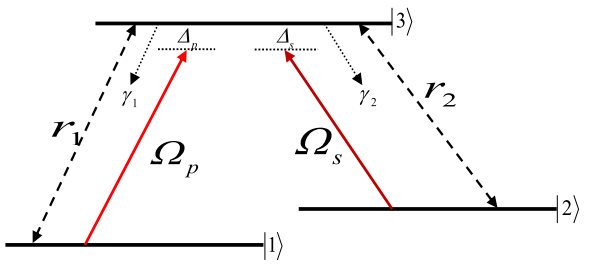

FIG. 5. Schematic of three-level Λ-type quantum system with closely spaced ground states. r_1 and r_2 are pump rates; Ω_p and Ω_s are the probe and signal fields.

In the above equations we have set $r_1 = r_2 = r$, and $\gamma_1 = \gamma_2 = \gamma$. We assume the weak-field approximation. We also consider that the three-level system is initially populated in the ground state $|1\rangle$, i.e., $\rho_{11}^{(0)} = 1$. After using the perturbation expansion featured in Eq. (9), the off-diagonal matrix elements of the first order $\rho_{31}^{(1)}$ and $\rho_{32}^{(1)}$ for the corresponding probe and signal transitions in their resonance conditions are given as follows:

$$\rho_{31}^{(1)} = \frac{4i\Delta}{4\Delta^2 - \eta^2 r^2}\Omega_p, \tag{20a}$$

$$\rho_{32}^{(1)} = -\frac{2i\eta r}{4\Delta^2 - \eta^2 r^2}\Omega_p, \tag{20b}$$

where $\Delta = \frac{1}{2}(2\gamma + 3r)$. Under the slowly varying envelope approximation and assuming time-independent fields, the following expressions for the propagation of weak fields Ω_p and Ω_s are obtained, when we assume at the beginning of the atomic cloud $(Z = 0)$ $\Omega_p(Z = 0) = \Omega_p(0)$ and $\Omega_s(Z = 0) = 0$:

$$\Omega_s(Z) = \Omega_p(0)\frac{\eta r}{2\gamma + 3r}\left[\exp\left(-\frac{\alpha Z}{L}\frac{(2\gamma + 3r)}{(2\gamma + 3r)^2 - \eta^2 r^2}\right) - 1\right], \tag{21a}$$

$$\Omega_p(Z) = \Omega_p(0)\exp\left(-\frac{\alpha Z}{L}\frac{(2\gamma + 3r)}{(2\gamma + 3r)^2 - \eta^2 r^2}\right). \tag{21b}$$

Clearly, the generated signal beam acquires again the same vorticity as that of the probe field. Figure 6 shows the dependence of the dimensionless intensities $|\Omega_s|^2/|\Omega_p(0)|^2$ and $|\Omega_p|^2/|\Omega_p(0)|^2$ on the dimensionless distance $\alpha Z/L$ for different values of quantum interference η. The absence of quantum interference results in zero exchange efficiency, indicating no OAM transfer between the probe and signal fields. The OAM exchange takes place in the presence of quantum interference term, and for $\eta = 1$ the exchange efficiency reaches to its maximum value [Fig. 6(a)]. Comparing to the V-type system, the generated signal beam does not oscillate now on propagation and the beam experiences no absorption loss for large propagation distances. The probe field will soon be absorbed by the medium, as observed in Fig. 6(b).

The effect of incoherent pumping rate on variation in space of probe and signal beams is illustrated in Fig. 7 for the case that the quantum interference is unity. As displayed in Fig. 7(a), the exchange efficiency increases by enhancing the incoherent pumping rate. On the other hand, the probe vortex suffers less absorption effects during the propagation for larger incoherent pumping rates. Therefore, adjusting together the incoherent pumping rate and quantum interference term provides a control in order to enhance the exchange efficiency.

Next, we show in Fig. 8 the exchange efficiency versus optical depth α for different value of incoherent pumping field for maximum value of quantum interference term. As can be seen, the larger the incoherent pumping rate and the optical depth, the larger the exchange efficiency, and the smaller the absorption losses.

C. Inhomogeneous medium

Inhomogeneous broadening of the transition lines in an atomic system is an important peculiarity, and even at low temperature, its magnitude is several orders wider than the

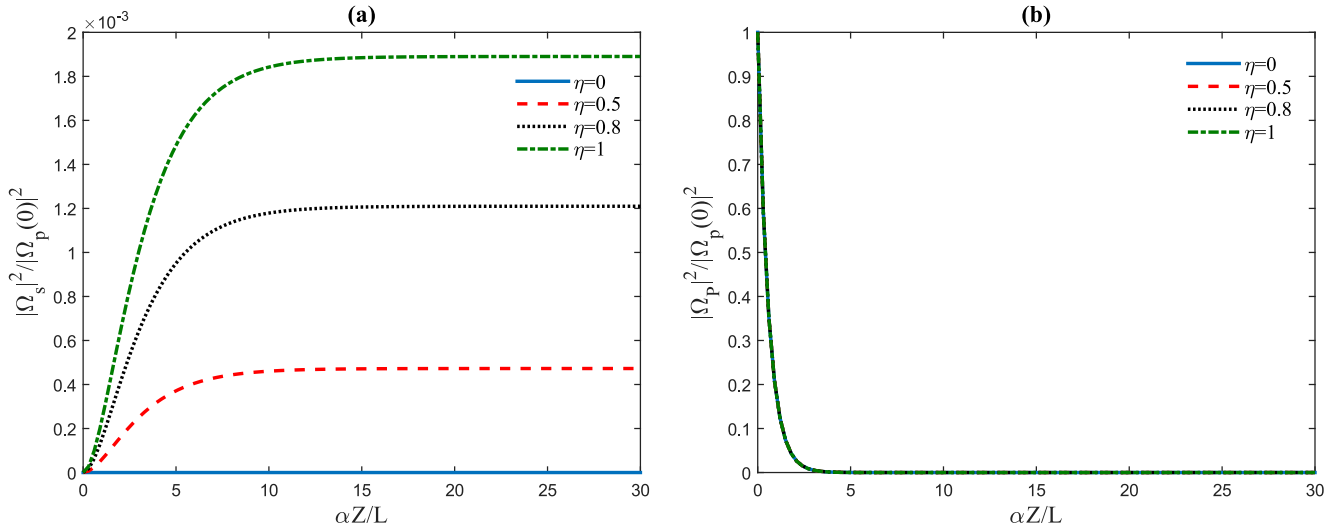

FIG. 6. The dependence of the dimensionless intensity of the signal field $|\Omega_s|^2/|\Omega_p(0)|^2$ (a) and probe field $|\Omega_p|^2/|\Omega_p(0)|^2$ (b) on the dimensionless distance $\alpha Z/L$. The selected parameters are $\gamma = 1\gamma$, $\alpha = 30$, $r = .1\gamma$, $\Delta_p = \Delta_s = 0$.

transition linewidth [44]. The optical fields experience different detunings due to inhomogeneous broadening. The detunings can be read as $\tilde{\Delta}_p = \Delta_p - \Delta_{ih}$, $\tilde{\Delta}_s = \Delta_s - \Delta_{ih}$, where $\Delta_{ih} = \omega_{31} - \tilde{\omega}_{31}$ and $\tilde{\omega}_{31}$ is the mean transition frequency. The off-diagonal matrix elements in both systems featured by Eqs. (11a), (11b) and (20a), (20b), in the presence of inhomogeneous broadening can be calculated by taking their averages over Δ_{ih} as follows:

$$\left\langle \rho_{m1}^{(1)}(\Delta_{ih}) \right\rangle = \int_{-\infty}^{\infty} f(\Delta_{ih}) \rho_{m1}^{(1)}(\Delta_{ih}) d\Delta_{ih}, \tag{22}$$

where $m = 3, 2$ and $f(\Delta_{ih})$ is the Gaussian distribution function given by

$$f(\Delta_{ih}) = \frac{1}{\sqrt{2\pi}\Gamma} e^{-\frac{\Delta_{ih}^2}{2\Gamma^2}}, \tag{23}$$

where Γ is the full width at half maximum.

We plot in Fig. 9 the dimensionless intensity of the signal field $|\Omega_s|^2/|\Omega_p(0)|^2$ versus $\alpha Z/L$ for homogeneous and inhomogeneous media for V type (a) and Λ type (b). We realize that the efficiency decreases in both cases when the inhomogeneous broadening is taken into account.

D. Effect of phase mismatch

Thus far our discussion has been limited to the phase-matching condition ($\Delta\vec{k} = \vec{k}_p - \vec{k}_s = 0$); however, experimentally it is difficult to ignore the phase-mismatch effect ($\Delta\vec{k} \neq 0$). In order to include the phase-mismatch effect in the proposed V model, Eq. (12b) is modified as [45]

$$\frac{\partial \Omega_s}{\partial Z} + i\Delta k \Omega_s = \frac{i\alpha_s \gamma}{2L}[a_2\Omega_p + b_2\Omega_s]. \tag{24}$$

The solution for Ω_s can be obtained by solving Eqs. (24) and (12a) with boundary conditions $\Omega_p(Z = 0) = \Omega_p(0)$ and

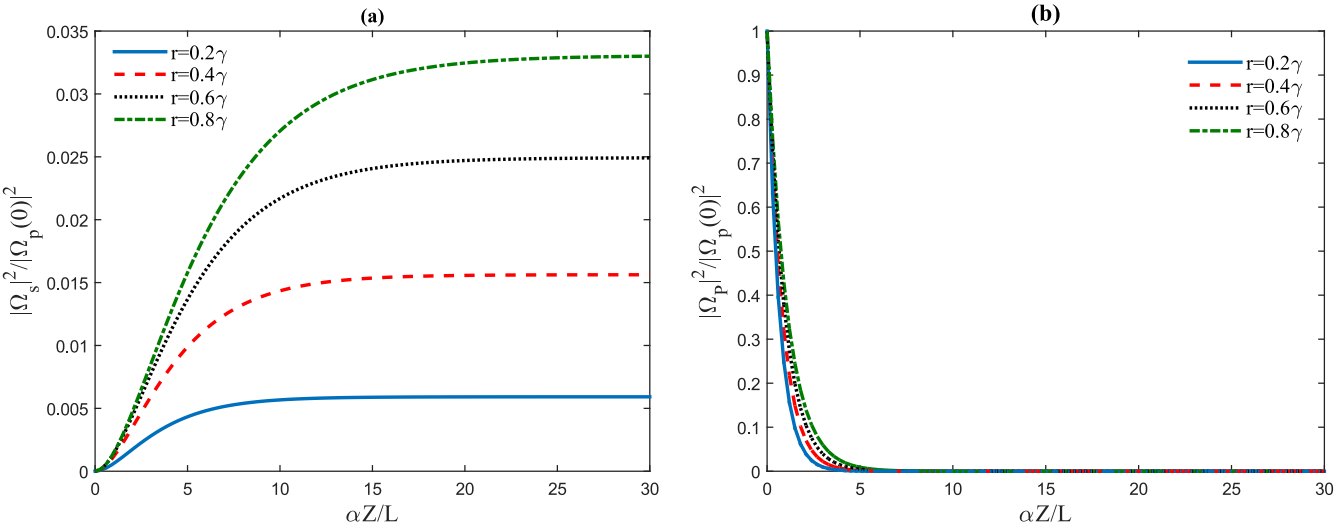

FIG. 7. The dependence of the dimensionless intensity of the signal field $|\Omega_s|^2/|\Omega_p(0)|^2$ (a) and probe field $|\Omega_p|^2/|\Omega_p(0)|^2$ (b) on the dimensionless distance $\alpha Z/L$. The selected parameters are $\gamma = 1\gamma$, $\alpha = 30$, $\eta = 1$, $\Delta_p = \Delta_s = 0$.

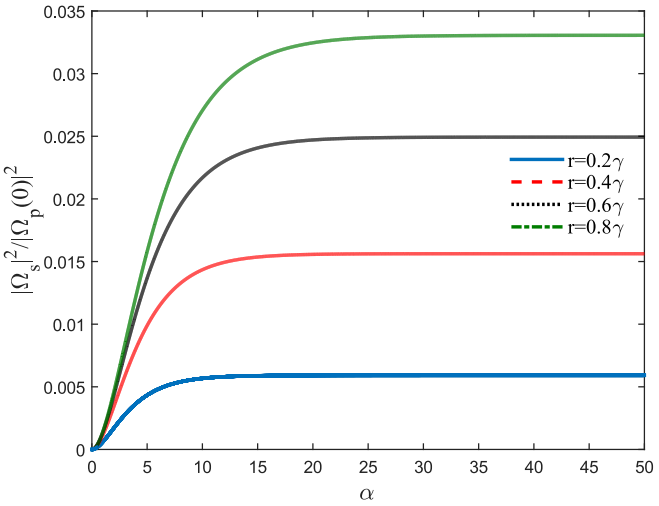

FIG. 8. The dependence of the dimensionless intensity of the signal field $|\Omega_s|^2/|\Omega_p(0)|^2$ on the optical depth α. The selected parameters are $Z = L,\ \eta = 1,\ \Delta_p = \Delta_s = 0$.

$\Omega_s(Z = 0) = 0$, giving

$$\Omega_s(Z) = \frac{A_2}{A_{PM}}\Omega_p(0)\left[e^{\frac{A_{PM}}{4L}Z} - e^{-\frac{A_{PM}}{4L}Z}\right]e^{(\frac{B_{PM}}{4L}Z)}, \qquad (25)$$

where $B_{PM} = A_1 + B_2 - 2i\Delta kL$, and $A_{PM} = A = \sqrt{(A_1 - B_2 + 2i\Delta kL)^2 + 4A_2B_1}$. If the incident weak field Ω_p is at angle θ, then we can define the phase-mismatch condition as $\Delta\vec{k} = (\vec{k}_p - \vec{k}_s)\cos\theta$, with $|\vec{k}_{p(s)}| = (n_{p(s)}\omega_{p(s)})/c$. To consider dispersion of the generated field, we select $n_s = 1 + 1/2\mathrm{Re}[\rho_{31}^{(1)}]$ and $n_p = 1$. The value of $\Delta\vec{k}$ then becomes [46]

$$\Delta\vec{k} = \frac{1}{c}\left((\omega_p - \omega_s)\cos\theta - \frac{\omega_s}{2}\mathrm{Re}\left[\rho_{31}^{(1)}\right]\right). \qquad (26)$$

In order to investigate the influence of phase mismatch on the exchange efficiency of OAM transfer, we plot the exchange efficiency versus ΔKL for homogeneous (a) and inhomogeneous (b) broadening for the V-type scheme in Fig. 10.

We observe that not only phase-mismatch effect reduces the OAM conversion efficiency, the effect becomes even more significant for the case of inhomogeneous broadening medium [Fig. 10(b)]. Similar results can be obtained for the Λ-type EIT medium.

III. SUMMARY

In summary, we have considered propagation of optical vortices in three-level V- and Λ-type atomic systems via noise-induced coherence created by the quantum interference from incoherent pumping field. In the V configuration, the system is initially prepared in its ground state while in the Λ-type scheme the system is initially in an EIT condition. We have realized that the exchange of optical vortices is possible in two different situations when the quantum interference is present. In both cases a generated signal field can obtain the same OAM as the vortex probe light during the propagation. The exchange efficiency of optical vortices is higher in the V-type system; however, the losses are always present. The losses are absent on propagation for the case of the Λ system, and one can control and even enhance the efficiency by properly adjusting the quantum interference term as well as the incoherent pumping rate. We have also considered the effects of phase mismatching and inhomogeneous broadening on exchange efficiency of vortex light.

ACKNOWLEDGMENTS

This project has received funding from European Social Fund (Project No. 09.3.3-LMT-K-712-19-0031) under grant agreement with the Research Council of Lithuania (LMTLT) for H.R.H.

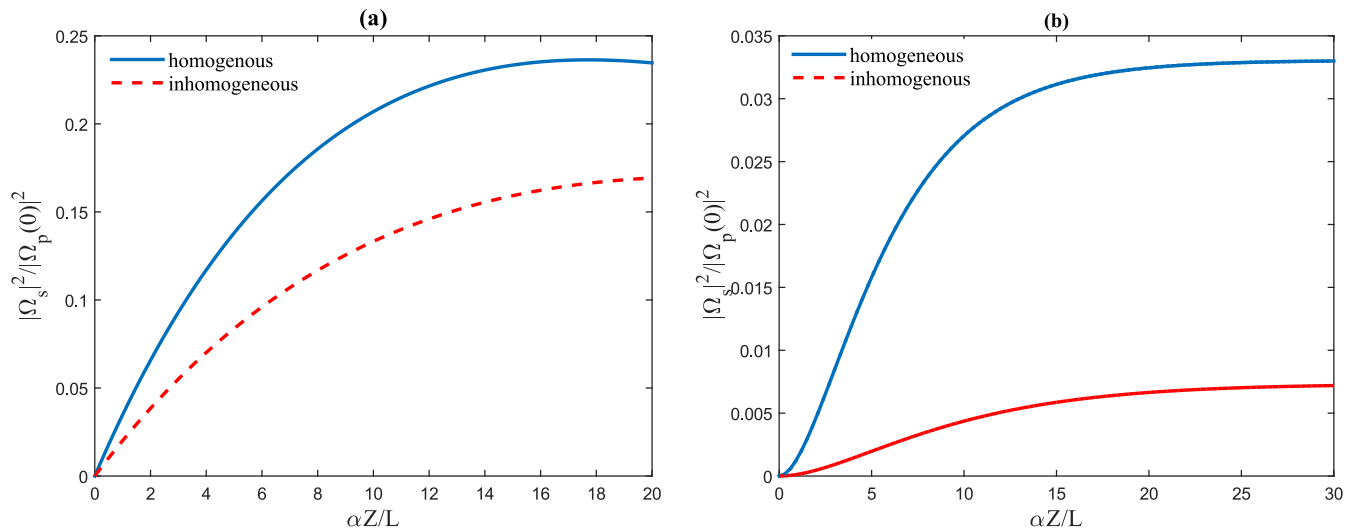

FIG. 9. The dependence of the dimensionless intensity of the signal field $|\Omega_s|^2/|\Omega_p(0)|^2$ on the dimensionless distance $\alpha Z/L$, for V-type (a), and Λ-type (b) atomic systems. Solid line corresponds to inhomogeneous and dashed line corresponds to inhomogeneous broadening. The selected parameters are for (a) $\alpha = 20,\ \eta = 1,\ \Delta_p = \Delta_s = 0,\ r = 6\gamma$, (b) $\alpha = 30,\ \eta = 1,\ \Delta_p = \Delta_s = 0,\ r = 0.8\gamma$.

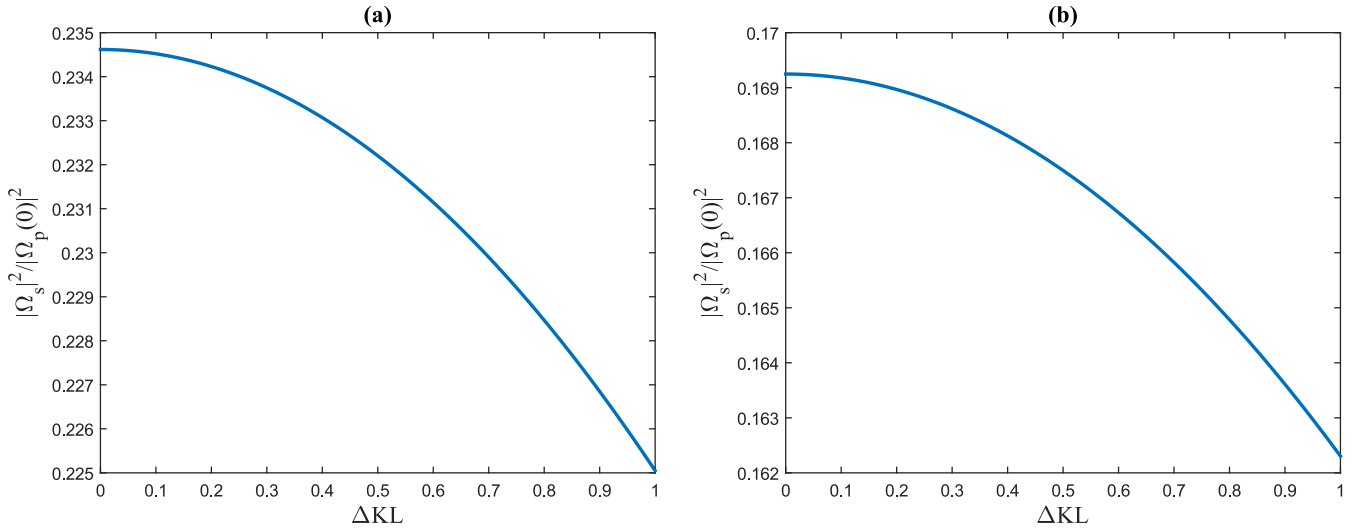

FIG. 10. Exchange efficiency of OAM vs phase mismatch in homogeneous (a) and inhomogeneous broadening (b) for V-type atomic system. The selected parameters are $\alpha = 20, \eta = 1,\ \Delta_p = \Delta_s = 0, r = 6\gamma,\ Z = L$.

APPENDIX A: DERIVATION OF INTERFERENCE TERMS FOR THE DECAY RATES FOR V-TYPE ATOMIC SYSTEM

In this Appendix, we study the impact of the Hamiltonian H_γ on the density-matrix elements. Let us consider all the three-levels without the presence of the pumping terms. The coupling of the atomic system due to vacuum reservoir is described by Eq. (5). In the interaction picture, one can characterize the Liouville equation for the total density operator ρ_T of the system (atom+reservoir) as

$$\dot{\rho}_T = -\frac{i}{\hbar}[H_\gamma(t), \rho_T(t)]. \tag{A1}$$

By integrating this equation once and replacing the result in it, we get

$$\dot{\rho}_T = -\frac{i}{\hbar}[H_\gamma(t), \rho_T(0)] + \left(i/\hbar^2\right)\int_0^t dt'[H_\gamma(t), [H_\gamma(t'), \rho_T(t')]], \tag{A2}$$

where the initial conditions are

$$\rho_T(0) = \rho^\gamma(0)\rho_F, \quad \rho_F \equiv \langle\{0_k\}||\{0_k\}\rangle. \tag{A3}$$

Here, $\rho^\gamma(0)$ describes the atomic density operator at $t = 0$, ρ_F characterizes the field density operator, and $|\{0_k\}\rangle$ represents the vacuum state. Since the reservoir is assumed to be a large extended open system characterized by many degrees of freedom and weakly coupled to the atom, the total density operator can be factorized into the product

$$\rho_T = \rho^\gamma(t)\rho_F \tag{A4}$$

for any $t > 0$. Such a factorization allows calculating the partial trace over the reservoir degrees of freedom, enabling formulation of equations of motion for the atomic density matrix. It follows then that the density-matrix element $\rho_{21}^{(\gamma)}$ satisfies the motion equation:

$$\dot{\rho}_{21}^{(\gamma)} = -\int_0^t dt' \sum_k g_k^{(1)2} \exp[i\nu_k(t-t')]\rho_{21}^\gamma(t') = -\int_0^t dt' \sum_k g_k^{(1)} g_k^{(2)} \exp[i\nu_k t - i\nu_k t')]\rho_{31}^\gamma(t'). \tag{A5}$$

Following the Wigner-Weisskopf approximation [16],

$$\sum_k \ldots \to \int_{-\infty}^{\infty} d\nu_k D(\nu_k)\ldots, \tag{A6}$$

and on interchanging the integrations over ν_k and t', one gets

$$\dot{\rho}_{21}^{(\gamma)} = -\int_0^t dt' \int_{-\infty}^{\infty} d\nu_k D(\nu_k) g_k^{(1)}\{g_k^{(1)}\rho_{21}^{(\gamma)}(t) \times \exp[i\nu_k(t-t')] + g_k^{(2)}\rho_{31}^{(\gamma)}(t')\exp(i\nu_k t) \times \exp(i\nu'_k t')\}, \tag{A7}$$

where

$$D(\nu_k) = \frac{V\nu_k^2}{\pi^2 c^3} \tag{A8}$$

shows the density of states while V stands for the quantization volume. If one considers that both atomic states $|3\rangle$ and $|2\rangle$ are close to each other, then the density of states $D(\nu_k)$ and the coupling constants $g_k^{(1)}$ and $g_k^{(2)}$ can contribute significantly only around $\nu_k = \omega$. As a result, ν_k can be replaced by ω in the corresponding terms, giving

$$\dot{\rho}_{21}^{(\gamma)} = -D(\omega)g_\omega^{(1)}\int_0^t dt' \int_{-\infty}^{\infty} d\nu_k\{g_k^{(1)}\rho_{21}^{(\gamma)}(t) \times \exp[i\nu_k(t-t')] + g_k^{(2)}\rho_{21}^{(\gamma)}(t')\exp(i\nu_k t) \times \exp(i\nu'_k t')\}, \tag{A9}$$

where after carrying out the integration

$$\dot{\rho}_{21}^{(\gamma)} = -\frac{1}{2}\gamma_2\rho_{21}^{(\gamma)} - \frac{1}{2}\sqrt{\gamma_1\gamma_2}\rho_{31}^{(\gamma)}, \tag{A10}$$

with $\gamma_1 = 2\pi D(\omega)g_\omega^{(1)2}$, $\gamma_2 = 2\pi D(\omega)g_\omega^{(2)2}$. It should be pointed out that both coupling constants are assumed to be positive. Following the same approach will lead to

$$\dot{\rho}_{31}^{(\gamma)} = -\frac{1}{2}\gamma_1\rho_{31}^{(\gamma)} - \frac{1}{2}\sqrt{\gamma_1\gamma_2}\rho_{21}^{(\gamma)}. \tag{A11}$$

Clearly, the terms containing the product of γ_1 and γ_2 characterize the quantum interference induced by the decay rates. Note that we ignore this type of noise-induced coherence in this paper, as we are interested here only in the effect of quantum interference induced by incoherent pumping process on our results. Therefore, we have

$$\dot{\rho}_{21}^{(\gamma)} = -\tfrac{1}{2}\gamma\rho_{21}^{(\gamma)}, \quad \dot{\rho}_{31}^{(\gamma)} = -\tfrac{1}{2}\gamma\rho_{31}^{(\gamma)}, \tag{A12}$$

as presented in Eq. (7).

APPENDIX B: DERIVATION OF INTERFERENCE TERM FROM THE INCOHERENT PUMPING FIELD FOR V-TYPE ATOMIC SYSTEM

In the following appendix, we provide a detailed analysis on noise-induced coherences created by the quantum interference of incoherent pumping rates, which is described by the Hamiltonian given in Eq. (3).

The Liouville equation for the density-matrix equations becomes

$$\dot{\rho}^{(R)} = -\frac{i}{\hbar}[H^{(R)},\ \rho^{(R)}] = -\frac{i}{\hbar}(H^{(R)}\rho^{(R)} - \rho^{(R)}H^{(R)}). \tag{B1}$$

Expanding Eq. (B1) yields

$$\begin{aligned}
\dot{\rho}_{31}^{(R)} &= -\frac{i}{\hbar}R\big[\mu_{31}\big(\rho_{33}^{(R)} - \rho_{11}^{(2)}\big) + \mu_{21}\rho_{32}^{(R)}\big],\\
\dot{\rho}_{21}^{(R)} &= -\frac{i}{\hbar}R\big[\mu_{21}\big(\rho_{22}^{(R)} - \rho_{11}^{(2)}\big) + \mu_{31}\rho_{23}^{(R)}\big],\\
\dot{\rho}_{32}^{(R)} &= -\frac{i}{\hbar}\big[\mu_{21}R^*\rho_{31}^{(R)} - \mu_{31}R\rho_{12}^{(R)}\big],\\
\dot{\rho}_{11}^{(R)} &= \frac{i}{\hbar}R^*\big[\mu_{21}\rho_{21}^{(R)} + \mu_{31}\rho_{31}^{(R)}\big] - \frac{i}{\hbar}R\big[\mu_{21}\rho_{12}^{(R)} + \mu_{31}\rho_{13}^{(R)}\big],\\
\dot{\rho}_{33}^{(R)} &= -\frac{i}{\hbar}\mu_{21}\big[R^*\rho_{21}^{(R)} - R\rho_{12}^{(R)}\big],\\
\dot{\rho}_{33}^{(R)} &= -\frac{i}{\hbar}\mu_{31}\big[R^*\rho_{31}^{(R)} - R\rho_{13}^{(R)}\big].
\end{aligned} \tag{B2}$$

Following a similar method as applied in Appendix A, we integrate these equations once and then replace them back into the above equation. Let us consider the density-matrix equation for the element $\rho_{31}^{(R)}$. We will require expressions for $\rho_{33}^{(R)}(t)$, $\rho_{11}^{(R)}(t)$, and $\rho_{32}^{(R)}(t)$. After the formal integration these expressions are

$$\begin{aligned}
\rho_{33}^{(R)}(t) &= -\frac{i}{\hbar}\mu_{21}\int_0^t d\tau\big[R^*(\tau)\rho_{21}^{(R)}(\tau) - R(\tau)\rho_{12}^{(R)}(\tau)\big],\\
\rho_{11}^{(R)}(t) &= \frac{i}{\hbar}\int_0^t d\tau R^*(\tau)\big[\mu_{21}\rho_{21}^{(R)}(\tau) + \mu_{31}\rho_{31}^{(R)}(\tau)\big],\\
\rho_{32}^{(R)}(t) &= -\frac{i}{\hbar}\int_0^t d\tau\big[\mu_{21}R^*(\tau)\rho_{31}^{(R)}(\tau) - \mu_{31}R(\tau)\rho_{12}^{(R)}(\tau)\big].
\end{aligned} \tag{B3}$$

Substituting Eq. (B3) in the equation for $\dot{\rho}_{31}^{(R)}$ in B2, we arrive at

$$\begin{aligned}
\dot{\rho}_{31}^{(R)} = {} & 2\Big(\frac{i}{\hbar}\Big)^2\mu_{31}^2\int_0^t d\tau R(\tau)R^*(\tau)\rho_{31}^{(R)}(\tau)\\
& + \Big(\frac{i}{\hbar}\Big)^2\mu_{21}^2\int_0^t d\tau R(\tau)R^*(\tau)\rho_{31}^{(R)}(\tau)\\
& + \Big(\frac{i}{\hbar}\Big)^2\mu_{21}\mu_{31}\int_0^t d\tau R(\tau)R^*(\tau)\rho_{21}^{(R)}(\tau).
\end{aligned} \tag{B4}$$

Then, using the δ correlation of the pumping fields, we get

$$\dot{\rho}_{31}^{(R)} = -\frac{1}{2}(2r_1 + r_2)\rho_{31} - \frac{1}{2}\sqrt{r_1r_2}\rho_{21}, \tag{B5}$$

where

$$r_{1,2} = 2\big(\mu_{31,21}^2/\hbar^2\big)\Re. \tag{B6}$$

We can obtain the equations of the motion for the remaining matrix elements by following the same approach:

$$\dot{\rho}_{21}^{(R)} = -\frac{1}{2}(2r_2 + r_1)\rho_{21} - \frac{1}{2}\sqrt{r_1r_2}\rho_{31}. \tag{B7}$$

Note that the terms involving products of r_1 and r_2 correspond to interference between the pumping processes from two upper states to ground level.

[1] Y. Wu and X. Yang, Phys. Rev. A **71**, 053806 (2005).
[2] M. Fleischhauer, A. Imamoglu, and J. P. Marangos, Rev. Mod. Phys. **77**, 633 (2005).
[3] S. Y. Kilin, K. T. Kapale, and M. O. Scully, Phys. Rev. Lett. **100**, 173601 (2008).
[4] Y. Wu and X. Yang, Appl. Phys. Lett. **91**, 094104 (2007).
[5] W.-X. Yang, A.-X. Chen, R.-K. Lee, and Y. Wu, Phys. Rev. A **84**, 013835 (2011) .
[6] W.-X. Yang, A.-X. Chen, L.-G. Si, K. Jiang, X. Yang, and R.-K. Lee, Phys. Rev. A **81**, 023814 (2010).
[7] W.-X. Yang, T.-T. Zha, and R.-K. Lee, Phys. Lett. A **374**, 355 (2009).
[8] Y. Wu, J. Saldana, and Y. Zhu, Phys. Rev. A **67**, 013811 (2003).
[9] Y. Wu and X. Yang, Phys. Rev. A **70**, 053818 (2004).
[10] Y. Wu and X. Yang, Phys. Rev. B **76**, 054425 (2007).
[11] T. V. Tscherbul and P. Brumer, Phys. Rev. Lett. **113**, 113601 (2014).
[12] A. Dodin, T. V. Tscherbul, and P. Brumer, J. Chem. Phys. **145**, 244313 (2016).

[13] B.-Q. Ou, L.-M. Liang, and C.-Z. Li, Opt. Commun. **281**, 4940 (2008).
[14] M. Sahrai, S. H. Asadpour, and R. Sadighi-Bonabi, J. Lumin. **131**, 2395 (2011).
[15] V. V. Kozlov, Y. Rostovtsev, and M. O. Scully, Phys. Rev. A **74**, 063829 (2006).
[16] K. T. Kapale, M. O. Scully, S.-Y. Zhu, and M. S. Zubairy, Phys. Rev. A **67**, 023804 (2003).
[17] V. Holubec and T. Novotný, J. Low Temp. Phys. **192**, 147 (2018).
[18] C. Wang, D. Xu, H. Liu, and X. Gao, Phys. Rev. E **99**, 042102 (2019).
[19] S. Koyu, A. Dodin, P. Brumer, and T. V. Tscherbul, Phys. Rev. Res. **3**, 013295 (2021).
[20] L. Allen, M. Padgett, and M. Babiker, Prog. Opt. **39**, 291 (1999).
[21] M. Padgett, J. Courtial, and L. Allen, Phys. Today **57** (5), 35 (2004).
[22] S. Liu, Y. Lou, and J. Jing, Nat. Commun. **11**, 3875 (2020).
[23] J. Leach, B. Jack, J. Romero, A. K. Jha, A. M. Yao, S. Franke-Arnold, D. G. Ireland, R. W. Boyd, S. M. Barnett, and M. J. Padgett, Science **329**, 662 (2010).
[24] S. H. Kazemi and M. Mahmoudi, Laser Phys. Lett. **16**, 076001 (2019).
[25] V. E. Lembessis and M. Babiker, Phys. Rev. A **82**, 051402(R) (2010).
[26] M. Babiker, W. L. Power, and L. Allen, Phys. Rev. Lett. **73**, 1239 (1994).
[27] D. Moretti, D. Felinto, and J. W. R. Tabosa, Phys. Rev. A **79**, 023825 (2009).
[28] A. Mair, A. Vaziri, G. Weihs, and A. Zeilinger, Nature (London) **412**, 313 (2001).
[29] G. Walker, A. S. Arnold, and S. Franke-Arnold, Phys. Rev. Lett. **108**, 243601 (2012).
[30] H. R. Hamedi, J. Ruseckas, and G. Juzeliūnas, Phys. Rev. A **98**, 013840 (2018).
[31] J. Qiu, Z. Wang, D. Ding, Z. Huang, and B. Yu, Phys. Rev. A **102**, 033516 (2020).
[32] Z. Wang, Y. Zhang, E. Paspalakis, and B. Yu, Phys. Rev. A **102**, 063509 (2020).
[33] Rahmatullah, M. Abbas, Ziauddin, and S. Qamar, Phys. Rev. A **101**, 023821 (2020).
[34] S. H. Asadpour, E. Paspalakis, and H. R. Hamedi, Phys. Rev. A **103**, 063705 (2021).
[35] S. H. Asadpour, E. Faizabadi, V. Kudriašov, E. Paspalakis, and H. R. Hamedi, Eur. Phys. J. Plus **136**, 457 (2021).
[36] H. R. Hamedi, V. Kudriašov, J. Ruseckas, and G. Juzeliūnas, Opt. Express **26**, 28249 (2018).
[37] N. Radwell, T. W. Clark, B. Piccirillo, S. M. Barnett, and S. Franke-Arnold, Phys. Rev. Lett. **114**, 123603 (2015).
[38] J. Ruseckas, A. Mekys, and G. Juzeliūnas, Phys. Rev. A **83**, 023812 (2011).
[39] J. Ruseckas, G. Juzeliūnas, P. Öhberg, and S. M. Barnett, Phys. Rev. A **76**, 053822 (2007).
[40] R. Pugatch, M. Shuker, O. Firstenberg, A. Ron, and N. Davidson, Phys. Rev. Lett. **98**, 203601 (2007).
[41] D. J. Fulton, S. Shepherd, R. R. Moseley, B. D. Sinclair, and M. H. Dunn, Phys. Rev. A **52**, 2302 (1995).
[42] H. R. Hamedi, E. Paspalakis, G. Žlabys, G. Juzeliūnas, and J. Ruseckas, Phys. Rev. A **100**, 023811 (2019).
[43] H. R. Hamedi, G. Juzeliūnas, E. Paspalakis, and J. Ruseckas, Phys. Rev. A **99**, 033812 (2019).
[44] H.-T. Zhou, D.-W. Wang, D. Wang, J.-X. Zhang, and S.-Y. Zhu, Phys. Rev. A **84**, 053835 (2011).
[45] R. Heitz, H. Born, F. Guffarth, O. Stier, A. Schliwa, A. Hoffmann, and D. Bimberg, Phys. Rev. B **64**, 241305(R) (2001).
[46] P. Lunnemann and J. Mørk, J. Opt. Soc. Am. B **27**, 2654 (2010).